Arch Appl Mech (2015) 85:223–235
DOI 10.1007/s00419-014-0915-1

ORIGINAL

Vlado A. Lubarda

On the circumferential shear stress around circular and elliptical holes

Received: 16 May 2014 / Accepted: 3 September 2014 / Published online: 13 September 2014

Abstract The circumferential shear stress along the boundary of a traction-free circular hole in an infinite isotropic solid under antiplane shear is twice the circumferential shear stress along the corresponding circle in an infinite solid without a hole, under the same loading conditions. This result, originally derived by Lin et al. (Yielding, damage, and failure of anisotropic solids. EGF Publication, Mechanical Engineering Publications, London, 1990) by invoking the extended circle theorem of Milne-Thomson, is rederived in this paper using the Fourier series analysis, in the spirit of the original Kienzler and Zhuping (J Appl Mech 54:110–114, 1987) derivation of the plane strain result for the hoop stress around the hole. The formula is also deduced by the complex potential method, without explicitly invoking the extended circle theorem. The ratio of the circumferential stresses along the boundary of a noncircular hole and the congruent curve in a solid without a hole depends on the loading. For an elliptical hole in an infinite solid under remote loading σ^0_{xz}, this ratio is constant and equal to $1 + b/a$; under σ^0_{yz} it is equal to $1 + a/b$, where a and b are the semi-axes of the ellipse. These constant values coincide with the values of the stress concentration factor in the two cases. If σ^0_{xz} and σ^0_{yz} are both applied, the stress ratio varies along the boundary of the ellipse; a closed form expression for this variation is determined. The portions of the elliptical boundary along which the strain energy density is increased or decreased by the creation of the hole are determined for different types of loading and different aspect ratios of the ellipse. An analytical expression for the stress concentration factor is then obtained for any orientation of the ellipse relative to the applied load.

Keywords Antiplane strain · Circle theorem · Complex potential · Conformal mapping · Elliptical hole · Fourier series · Strain energy · Stress concentration factor

1 Introduction

There is a remarkable formula for hoop stress along the boundary of a circular hole in an infinite medium under plane stress or plane strain conditions, derived by Kienzler and Zhuping [2], which reads

Dedicated to the memory of the late Professor Vlatko Brčić from the University of Belgrade Department of Civil Engineering.

V. A. Lubarda (✉)
Departments of NanoEngineering and Mechanical and Aerospace Engineering, University of California, San Diego, La Jolla, CA 92093-0448, USA
Tel.: 858-534-3169
Fax: 858-534-5698
E-mail: vlubarda@ucsd.edu

V. A. Lubarda
Montenegrin Academy of Sciences and Arts, Rista Stijovića 5, 81000 Podgorica, Montenegro

$$\sigma_\theta(a,\theta) = 2\left[\sigma_\theta^0(a,\theta) - \sigma_r^0(a,\theta)\right] + \frac{1}{2}\left[\sigma_\theta^0(0,\theta) + \sigma_r^0(0,\theta)\right]. \tag{1}$$

The superscript '0' denotes the fields in an infinite medium without a hole, and (r,θ) are the polar coordinates with the origin at the center of the hole of radius $r = a$. The establishment of this formula stimulated research that led to the formulation of the so-called heterogenization procedure [3,4], according to which the solution of the problems of two or more inhomogeneities under remote or other type of loadings can be expressed in terms of the solution to the corresponding homogeneous problems. Less known is the formula for the circumferential shear stress along the boundary of a circular hole in the case of antiplane strain, according to which the circumferential shear stress is equal twice the circumferential shear stress along the corresponding circle in an infinite medium without a hole, under the same loading conditions. This formula was first noted by Lin et al. [1], who deduced it from the expressions for the stress components outside a circular inhomogeneity in an infinite medium,

$$\sigma_{zr}(r,\theta) = \sigma_{zr}^0(r,\theta) + \lambda\,\frac{a^2}{r^2}\,\sigma_{zr}^0\left(a^2/r,\theta\right), \quad \sigma_{z\theta}(r,\theta) = \sigma_{z\theta}^0(r,\theta) - \lambda\,\frac{a^2}{r^2}\,\sigma_{z\theta}^0\left(a^2/r,\theta\right). \tag{2}$$

The superposed '0' designates the stress field in a homogeneous infinite medium without the inhomogeneity, $\lambda = (\mu_\mathrm{I} - \mu_\mathrm{M})/(\mu_\mathrm{I} + \mu_\mathrm{M})$, and $(\mu_\mathrm{I}, \mu_\mathrm{M})$ are the shear moduli of the inhomogeneity and matrix, respectively. The stress field (2) follows from a version of the Milne-Thomson circle theorem for irrotational two-dimensional flow of an incompressible inviscid fluid [5,6]. According to this theorem, the complex potentials for the stress field inside and outside the inhomogeneity are $\omega_\mathrm{I}(z) = (1+\lambda)\omega^0(z)$ and $\omega_\mathrm{M}(z) = \omega^0(z) + \lambda\overline{\omega}^0(a^2/z)$, where $\omega^0(z)$ is the complex potential of the homogeneous problem without the inhomogeneity, for the same loading outside the circle $r = a$. The complex state of stress is $\sigma_{zy} + i\sigma_{zx} = \omega'(z)$, where the prime designates the derivative with respect to the complex variable z. The theorem was first applied to solid mechanics by Smith [7] to study the interaction between a screw dislocation and a circular inhomogeneity, and, independently, in a sequence of papers on inhomogeneities by Honein et al. [8–10], who referred to it as the extended circle theorem. If the inhomogeneity is a void ($\lambda = -1$), from the second equation of (2) follows that the circumferential shear stress along the boundary of the void is

$$\sigma_{z\theta}(a,\theta) = 2\sigma_{z\theta}^0(a,\theta), \tag{3}$$

which is the circumferential shear stress formula of Lin et al. [1].

While the plane strain formula (1) has been applied in [11] to evaluate the interaction between a circular hole and an edge dislocation, and has been discussed by others, e.g., [3,4,12–16], the antiplane strain formula (3) has not been previously used or cited in the literature, except in the author's own recent work [17], where it was used to evaluate the configurational forces in the problem of a circular inclusion subjected to an eigenstrain near a traction-free circular void. It seems, therefore, desirable to shed additional light to this formula, which is accomplished here using the Fourier series analysis, similarly to the Kienzler and Zhuping [2] derivation of the plane strain formula. It is also derived using the complex variables approach, without explicitly invoking the extended circle theorem. In contrast to circular holes, the ratio of the circumferential shear stress along the boundary of a noncircular hole and the congruent curve in an unweakened solid depends on the loading. For an elliptical hole in a solid under remote loading σ_{xz}^0, this ratio is constant and equal to $1 + b/a$; under σ_{yz}^0 it is equal to $1 + a/b$, where a and b are the semi-axes of the ellipse. These constant values coincide with the values of the stress concentration factor in the two cases. If σ_{xz}^0 and σ_{yz}^0 are applied, the ratio varies along the boundary of the ellipse. The expression for this variation is derived. The change in the strain energy density (its increase or decrease) along the boundary of the ellipse, due to creation of the elliptical hole, is determined for different types of loading and different aspect ratios of the ellipse. A closed form expression for the stress concentration factor is then obtained for an arbitrary orientation of the ellipse relative to the applied load.

2 Circumferential shear stress along the boundary of the hole

Consider a traction-free circular cylindrical hole of radius a in an infinitely extended isotropic elastic solid (Fig. 1). Suppose that at point C, at the distance d from the center O of the hole, there exists a source of stress, such as a screw dislocation or a line force along direction parallel to the z-axis. The source of stress can also be a circular inclusion of radius $b \le (d - a)$, centered at point C and characterized by uniform antiplane eigenshear. Alternatively, the source of stress can be a remote antiplane shear loading. The nonvanishing stress

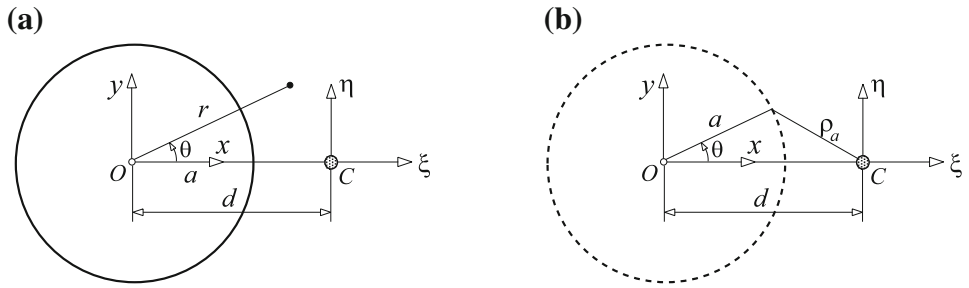

Fig. 1 **a** The source of stress at point C at a distance d from the center of the traction-free hole of radius a. The polar coordinates from the origin O are (r, θ). The cartesian coordinates centered at O are (x, y), while those centered at C are (ξ, η). **b** The source of stress at point C in an infinite solid without the hole. The *dashed-line* circle is of radius a, coincident with the boundary of the hole from part (**a**). The distance from C to an arbitrary point on the circle is ρ_a

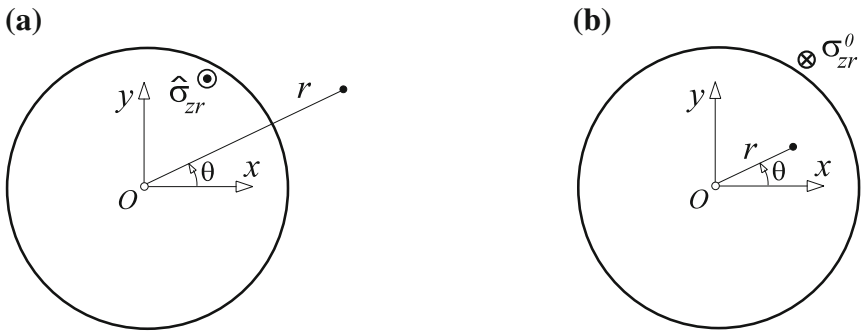

Fig. 2 **a** The auxiliary problem in which the hole in an infinite medium is loaded over its boundary $r = a$ with self-equilibrating traction $\hat{\sigma}_{zr}(a, \theta) = -\sigma^0_{zr}(a, \theta)$, where $\sigma^0_{zr}(a, \theta)$ is the radial shear stress component along the circle $r = a$ in an infinite medium without a hole. **b** Solid circular cylinder loaded over its boundary $r = a$ by the shear stress $\sigma^0_{zr}(a, \theta)$

components in antiplane strain problems are σ_{zr} and $\sigma_{z\theta}$, where (r, θ) are the indicated polar coordinates. Along the traction-free boundary of the circular hole, $\sigma_{rz} = 0$ (the other two traction components, σ_{rr} and $\sigma_{r\theta}$, being also equal to zero). The shear stresses are related to shear strains $\epsilon_{zr} = (1/2)\partial w/\partial r$ and $\epsilon_{z\theta} = (1/2r)\partial w/\partial\theta$ by Hooke's law as $\sigma_{zr} = 2\mu\epsilon_{zr}$ and $\sigma_{z\theta} = 2\mu\epsilon_{z\theta}$, where $w = w(r, \theta)$ is the nonvanishing out-of-plane displacement component. Thus, $\sigma_{zr} = \partial\Phi/\partial r$ and $\sigma_{z\theta} = r^{-1}\partial\Phi/\partial\theta$, with $\Phi = \Phi(r, \theta) = \mu w(r, \theta)$ as the stress function. The substitution into equilibrium equation gives the governing Laplace's equation for Φ,

$$\frac{\partial}{\partial r}(r\sigma_{zr}) + \frac{\partial\sigma_{z\theta}}{\partial\theta} = 0 \Rightarrow \frac{\partial^2\Phi}{\partial r^2} + \frac{1}{r}\frac{\partial\Phi}{\partial r} + \frac{1}{r^2}\frac{\partial^2\Phi}{\partial\theta^2} = 0. \tag{4}$$

The stress field around a hole due to the source of stress at C can be determined by superposition. First, the stress distribution $\sigma^0_{zr}(r, \theta)$ and $\sigma^0_{z\theta}(r, \theta)$ is found in an infinite medium without a hole due to the same source of stress (Fig. 1b). Second, the auxiliary problem is solved for the hole in an infinite medium, loaded on its surface $r = a$ by self-equilibrating (image) traction $\hat{\sigma}_{zr}(a, \theta) = -\sigma^0_{zr}(a, \theta)$, as sketched in Fig. 2a. The stress distribution of the original problem from Fig. 1a is the sum of the stress distributions for problems from Figs. 1b and 2a, i.e.,

$$\sigma_{zr}(r, \theta) = \sigma^0_{zr}(r, \theta) + \hat{\sigma}_{zr}(r, \theta), \quad \sigma_{z\theta}(r, \theta) = \sigma^0_{z\theta}(r, \theta) + \hat{\sigma}_{z\theta}(r, \theta). \tag{5}$$

2.1 Fourier series for $\sigma^0_{zr}(a, \theta)$ and $\sigma^0_{z\theta}(a, \theta)$

The Fourier series for the stress component $\sigma^0_{zr}(a, \theta)$ around the circle $r = a$ is

$$\sigma^0_{zr}(a, \theta) = \sum_{n=1}^{\infty}\left(A^0_n\cos n\theta + B^0_n\sin n\theta\right), \quad \sigma^0_{z\theta}(a, \theta) = \sum_{n=1}^{\infty}\left(B^0_n\cos n\theta - A^0_n\sin n\theta\right), \tag{6}$$

where A_n^0 and B_n^0 are the corresponding Fourier coefficients. In proof of (6), consider a circular cylinder of radius a loaded on its boundary by the shear stress $\sigma_{zr}^0(a,\theta)$, as shown in Fig. 2b. The stress state in this cylinder is the same as the state of stress inside the circle $r = a$ of the infinite medium problem from Fig. 1b. The stress function for the cylinder problem is

$$\Phi_{\rm c}(r,\theta) = \sum_{n=1}^{\infty} r^n (A_n \cos n\theta + B_n \sin n\theta), \tag{7}$$

such that

$$\begin{aligned} \sigma_{zr}^0(r,\theta) &= \frac{\partial \Phi_{\rm c}}{\partial r} = \sum_{n=1}^{\infty} n r^{n-1}(A_n \cos n\theta + B_n \sin n\theta), \\ \sigma_{z\theta}^0(r,\theta) &= \frac{1}{r}\frac{\partial \Phi_{\rm c}}{\partial \theta} = \sum_{n=1}^{\infty} n r^{n-1}(B_n \cos n\theta - A_n \sin n\theta). \end{aligned} \tag{8}$$

Along the boundary of the cylinder, these stresses become

$$\begin{aligned} \sigma_{zr}^0(a,\theta) &= \sum_{n=1}^{\infty} n a^{n-1}(A_n \cos n\theta + B_n \sin n\theta), \\ \sigma_{z\theta}^0(r,\theta) &= \sum_{n=1}^{\infty} n a^{n-1}(B_n \cos n\theta - A_n \sin n\theta). \end{aligned} \tag{9}$$

The identifications $na^{n-1}A_n = A_n^0$ and $na^{n-1}B_n = B_n^0$ prove (6).

2.2 Auxiliary problem

The stress field due to self-equilibrating traction $\hat{\sigma}_{zr}(a,\theta) = -\sigma_{zr}^0(a,\theta)$ must vanish as $r \to \infty$. The appropriate stress function for the auxiliary problem from Fig. 2a is thus

$$\hat{\Phi}(r,\theta) = \sum_{n=1}^{\infty} r^{-n}\left(\hat{A}_n \cos n\theta + \hat{B}_n \sin n\theta\right). \tag{10}$$

The corresponding stresses are

$$\begin{aligned} \hat{\sigma}_{zr}(r,\theta) &= \frac{\partial \hat{\Phi}}{\partial r} = -\sum_{n=1}^{\infty} n r^{-n-1}(\hat{A}_n \cos n\theta + \hat{B}_n \sin n\theta), \\ \hat{\sigma}_{z\theta}(r,\theta) &= \frac{1}{r}\frac{\partial \hat{\Phi}}{\partial \theta} = \sum_{n=1}^{\infty} n r^{-n-1}(\hat{B}_n \cos n\theta - \hat{A}_n \sin n\theta). \end{aligned} \tag{11}$$

The boundary condition $\hat{\sigma}_{zr}(a,\theta) = -\sigma_{zr}^0(a,\theta)$ specifies the constants $\hat{A}_n$ and $\hat{B}_n$, such that $na^{-n-1}\hat{A}_n = A_n^0$ and $na^{-n-1}\hat{B}_n = B_n^0$. The substitution into (11), therefore, gives

$$\begin{aligned} \hat{\sigma}_{zr}(r,\theta) &= -\sum_{n=1}^{\infty}\left(\frac{a}{r}\right)^{n+1}(A_n^0 \cos n\theta + B_n^0 \sin n\theta), \\ \hat{\sigma}_{z\theta}(r,\theta) &= \sum_{n=1}^{\infty}\left(\frac{a}{r}\right)^{n+1}\left(B_n^0 \cos n\theta - A_n^0 \sin n\theta\right). \end{aligned} \tag{12}$$

The circumferential shear stress along the boundary of the hole is consequently

$$\hat{\sigma}_{z\theta}(a,\theta) = \sum_{n=1}^{\infty}\left(B_n^0 \cos n\theta - A_n^0 \sin n\theta\right). \tag{13}$$

The comparison of (13) with the second part of (6) thus establishes $\hat{\sigma}_{z\theta}(a,\theta) = \sigma^0_{z\theta}(a,\theta)$. The circumferential shear stress along the boundary of the hole of the original problem is $\sigma_{z\theta}(a,\theta) = \sigma^0_{z\theta}(a,\theta) + \hat{\sigma}_{z\theta}(a,\theta) = 2\sigma^0_{z\theta}(a,\theta)$, which is the Lin et al. [1] formula.

The same type of analysis can be performed in the case of an infinite medium with a hole under remote antiplane shear loading $(\sigma^0_{zx}, \sigma^0_{zy})$. The circumferential shear stress along the boundary of the hole is then

$$\sigma_{z\theta}(a,\theta) = 2\sigma^0_{z\theta}(a,\theta) = 2\left(\sigma^0_{zy}\cos\theta - \sigma^0_{zx}\sin\theta\right). \tag{14}$$

3 Derivation by the complex potential approach

The most general function analytic inside the cylinder due to self-equilibrating traction $\sigma^0_{zr}(t)$ over its boundary $z = t = a\exp(i\theta)$ is a complex polynomial

$$\omega(z) = \sum_{n=1}^{\infty}(B_n + iA_n)z^n, \quad z = r\exp(i\theta), \tag{15}$$

i.e., in an expanded form,

$$\omega(z) = \sum_{n=1}^{\infty} r^n\left[(B_n\cos n\theta - A_n\sin n\theta) + i\,(A_n\cos n\theta + B_n\sin n\theta)\right]. \tag{16}$$

The stresses in the cylinder are deduced from

$$\sigma^0 = \sigma^0_{zy} + i\sigma^0_{zx} = \omega'(z) = \sum_{n=1}^{\infty} n(B_n + iA_n)z^{n-1}, \tag{17}$$

with the polar coordinates representation

$$\tau^0 = \sigma^0_{z\theta} + i\sigma^0_{zr} = \sigma^0\exp(i\theta) = \sum_{n=1}^{\infty} n(B_n + iA_n)r^{n-1}\exp(in\theta). \tag{18}$$

Along the boundary of the cylinder, this gives

$$\tau^0(t) = \sum_{n=1}^{\infty} na^{n-1}\left[(B_n\cos n\theta - A_n\sin n\theta) + i\,(A_n\cos n\theta + B_n\sin n\theta)\right]. \tag{19}$$

The most general function analytic in an infinite medium outside the hole, due to self-equilibrating traction $\hat{\sigma}_{zr}(t) = -\sigma^0_{zr}(t)$ applied over the boundary of the hole, is

$$\hat{\omega}(z) = -\overline{\omega}\left(\frac{a^2}{z}\right) = -\sum_{n=1}^{\infty}(B_n - iA_n)\left(\frac{a^2}{z}\right)^n \tag{20}$$

yielding

$$\hat{\omega}(z) = \sum_{n=1}^{\infty}\left(\frac{a^2}{r}\right)^n\left[(A_n\sin n\theta - B_n\cos n\theta) + i(A_n\cos n\theta + B_n\sin n\theta)\right]. \tag{21}$$

The stresses are

$$\hat{\sigma} = \hat{\sigma}_{zy} + i\hat{\sigma}_{zx} = \hat{\omega}'(z) = \sum_{n=1}^{\infty} n(B_n - iA_n)\frac{a^{2n}}{z^{n+1}}, \tag{22}$$

with the polar coordinates representation

$$\hat{\tau} = \hat{\sigma}_{z\theta} + i\hat{\sigma}_{zr} = \hat{\sigma}\exp(i\theta) = \sum_{n=1}^{\infty} n(B_n - iA_n)\frac{a^{2n}}{r^{n+1}}\exp(-in\theta). \tag{23}$$

Along the boundary of hole, (23) gives

$$\hat{\tau}(t) = \sum_{n=1}^{\infty} n a^{n-1}[(B_n \cos n\theta - A_n \sin n\theta) - i(A_n \cos n\theta + B_n \sin n\theta)]. \tag{24}$$

By comparing (19) and (24), it follows that the stress state $\hat{\tau}(t)$ is the complex conjugate to the stress state $\tau^0(t)$, i.e., $\hat{\tau}(t) = \overline{\tau}^0(t)$. Consequently,

$$\hat{\sigma}_{zr}(a,\theta) = -\sigma^0_{zr}(a,\theta), \quad \hat{\sigma}_{z\theta}(a,\theta) = \sigma^0_{z\theta}(a,\theta). \tag{25}$$

Since the total stress of the original problem is the sum of the infinite-medium stress and the stress state from the auxiliary problem, we again establish the circumferential shear stress formula $\sigma_{z\theta}(a,\theta) = 2\sigma^0_{z\theta}(a,\theta)$.

4 Circumferential shear stress around elliptical hole

For noncircular holes, the ratio of the circumferential shear stresses along the boundary of the hole and along the congruent curve in a solid without a hole is dependent on the type of loading and varies along the boundary of the hole. This is demonstrated by considering an elliptical hole under remote shear loading σ^0_{xz} and σ^0_{yz}, shown in Fig. 3a. The corresponding stress field can be conveniently determined from the stress field around a circular hole by applying conformal mapping, e.g., [18]. The complex potential for the circular hole problem from Fig. 3b is

$$\Omega(\zeta) = \sigma^0_{yz}\left(\zeta - \frac{R^2}{\zeta}\right) + i\sigma^0_{xz}\left(\zeta + \frac{R^2}{\zeta}\right), \tag{26}$$

where $\zeta = \rho e^{i\varphi}$. The conformal mapping of the region outside the circle of radius $R = (a+b)/2$ in the complex ζ-plane to the region outside the ellipse with the semi-axes a and b in the complex z-plane is given in [19–21] as

$$z = \Gamma(\zeta) = \zeta + \frac{a^2 - b^2}{4\zeta}, \tag{27}$$

where $z = re^{i\theta}$. The stress components follow from

$$\sigma_{yz} + i\sigma_{xz} = \frac{\mathrm{d}\omega}{\mathrm{d}z} = \frac{\mathrm{d}\Omega/\mathrm{d}\zeta}{\mathrm{d}\Gamma/\mathrm{d}\zeta}, \tag{28}$$

which gives

$$\sigma_{yz} + i\sigma_{xz} = \frac{(\sigma^0_{yz} + i\sigma^0_{xz}) + (\sigma^0_{yz} - i\sigma^0_{xz})\dfrac{(a+b)^2}{4\zeta^2}}{1 - \dfrac{a^2 - b^2}{4\zeta^2}}. \tag{29}$$

Along the boundary of the hole the relation $\zeta = [(a+b)/2]\exp(i\varphi)$ is valid. Inserting it into (29) yields the shear stress components along the boundary of the ellipse as

$$\begin{aligned} \sigma_{xz} &= \frac{-(1+k)\sin\varphi}{\sin^2\varphi + k^2\cos^2\varphi}\left(\sigma^0_{yz}\cos\varphi - \sigma^0_{xz}\sin\varphi\right), \\ \sigma_{yz} &= \frac{k(1+k)\cos\varphi}{\sin^2\varphi + k^2\cos^2\varphi}\left(\sigma^0_{yz}\cos\varphi - \sigma^0_{xz}\sin\varphi\right). \end{aligned} \tag{30}$$

The aspect ratio of the ellipse is $k = b/a$. It can be readily verified that the traction-free condition along the boundary of the hole is satisfied, i.e., $\sigma_{nz} = \sigma_{xz}\sin\beta + \sigma_{yz}\cos\beta = 0$, where n is the direction orthogonal to the boundary of the elliptical hole at an arbitrary point of that boundary (Fig. 4).

The circumferential shear stress along the boundary of an elliptical hole and along the congruent ellipse in a solid without a hole are

$$\tau = \sigma_{yz}\sin\beta - \sigma_{xz}\cos\beta, \quad \tau^0 = \sigma^0_{yz}\sin\beta - \sigma^0_{xz}\cos\beta, \tag{31}$$

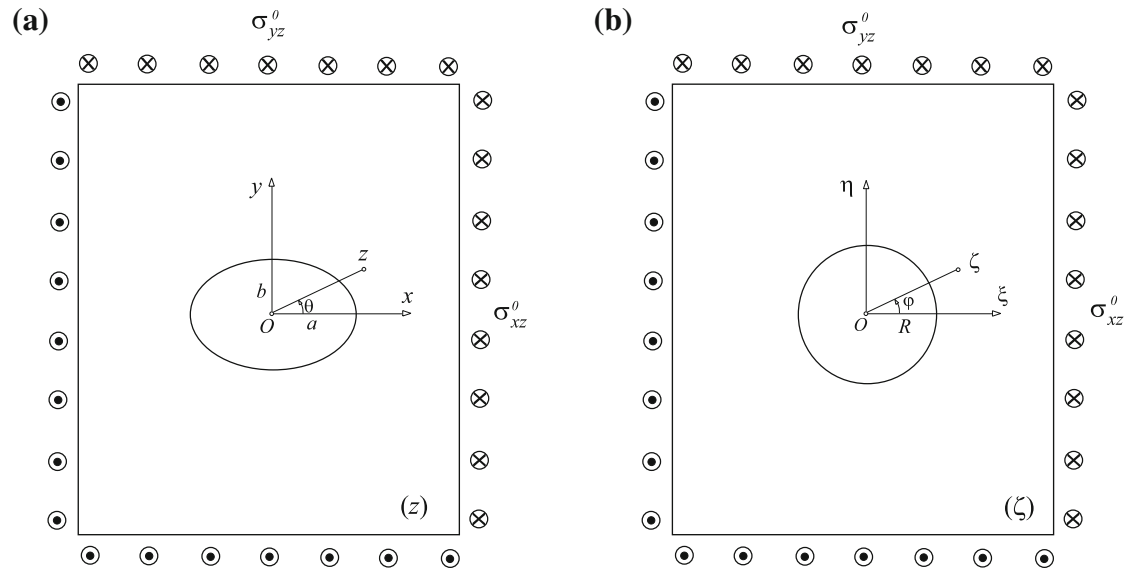

Fig. 3 **a** An infinite solid with an elliptical cylindrical hole with the semi-axes a and b. The applied remote antiplane shear stress components are σ^0_{xz} and σ^0_{yz}. **b** An infinite solid with a circular cylindrical hole of radius $R = (a + b)/2$. The remote antiplane shear stresses are the same as in part (**a**)

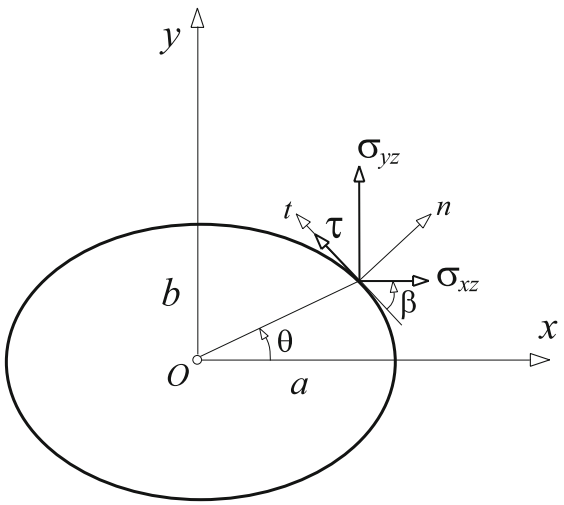

Fig. 4 The circumferential shear stress $\tau = \sigma_{yz} \sin\beta - \sigma_{xz} \cos\beta$ at an arbitrary point of the elliptical hole ($x = a\cos\varphi,\ y = b\sin\varphi$) in an infinite solid under remote antiplane shear stresses σ^0_{xz} and σ^0_{yz} is obtained by projecting the shear stress components σ_{xz} and σ_{yz} in the direction of the tangent t to the ellipse. The geometric relations hold $\tan\theta = k\tan\varphi,\ \tan\beta = k\cot\varphi$, where $k = b/a$. The elliptical hole is traction-free, so that $\sigma_{nz} = \sigma_{xz}\sin\beta + \sigma_{yz}\cos\beta = 0$, where n is the direction orthogonal to the boundary of the hole

with

$$\sin\beta = \frac{k\cos\varphi}{\left(\sin^2\varphi + k^2\cos^2\varphi\right)^{1/2}}, \quad \cos\beta = \frac{\sin\varphi}{\left(\sin^2\varphi + k^2\cos^2\varphi\right)^{1/2}} \tag{32}$$

from Fig. 4. The substitution of (32) into (31) gives

$$\tau = \frac{k\sigma_{yz}\cos\varphi - \sigma_{xz}\sin\varphi}{\left(\sin^2\varphi + k^2\cos^2\varphi\right)^{1/2}}, \quad \tau^0 = \frac{k\sigma^0_{yz}\cos\varphi - \sigma^0_{xz}\sin\varphi}{\left(\sin^2\varphi + k^2\cos^2\varphi\right)^{1/2}}. \tag{33}$$

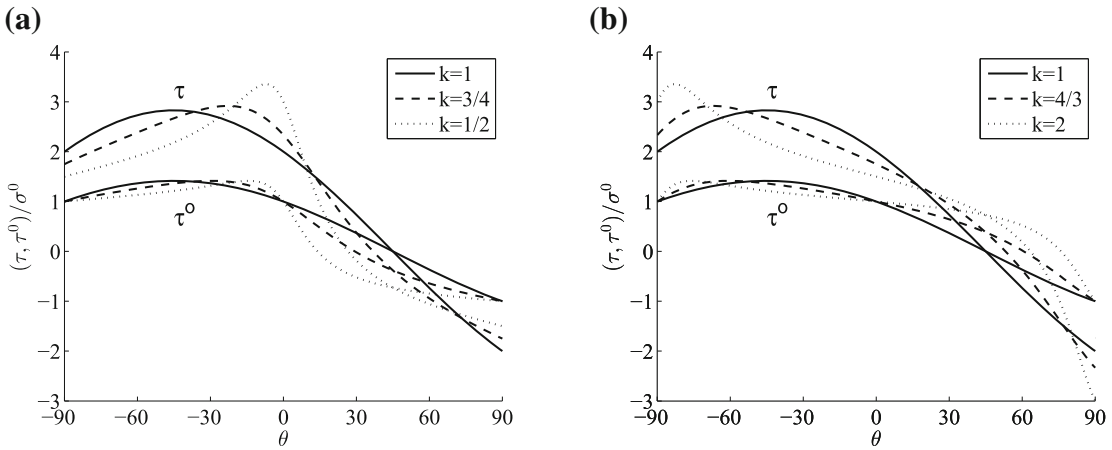

Fig. 5 The variation of the circumferential stresses τ and τ^0 under remote loading $\sigma^0_{xz} = \sigma^0_{yz} = \sigma^0$ (scaled by σ^0) along the ellipse for: **a** three selected values of the ellipse aspect ratio $k = b/a$, and **b** their reciprocals

When (30) is substituted into (33), the circumferential shear stress along the boundary of the elliptical hole becomes

$$\tau = (1+k)\,\frac{\sigma^0_{yz}\cos\varphi - \sigma^0_{xz}\sin\varphi}{\left(\sin^2\varphi + k^2\cos^2\varphi\right)^{1/2}}. \tag{34}$$

This is plotted in Fig. 5. Thus, the difference of the two circumferential stresses is

$$\tau - \tau^0 = \frac{\sigma^0_{yz}\cos\varphi - k\sigma^0_{xz}\sin\varphi}{(\sin^2\varphi + k^2\cos^2\varphi)^{1/2}}. \tag{35}$$

For $k \neq 1$, the ratio τ/τ^0 is dependent on φ and, thus, varies along the circumference of the ellipse. However, in the case of remote shear loading $\sigma^0_{yz} \neq 0,\ \sigma^0_{xz} = 0$, the ratio $\tau/\tau^0 = 1 + k^{-1}$ is constant along the boundary of the ellipse. It is also constant in the case of remote shear loading $\sigma^0_{xz} \neq 0,\ \sigma^0_{yz} = 0$, where $\tau/\tau^0 = 1 + k$. In both cases, the constant value is equal to the stress concentration factor of the solid weakened by the corresponding elliptical hole. If $\sigma^0_{yz} = \pm\sigma^0_{xz}$, one has

$$\frac{\tau - \tau^0}{\sigma^0_{yz}} = \frac{\cos(\varphi \pm \psi)}{(\sin^2\varphi + k^2\cos^2\varphi)^{1/2}}, \tag{36}$$

where the angle $\psi = \arctan(b/a)$.

The extreme value of the circumferential shear stress is obtained from the condition

$$\frac{\mathrm{d}\tau}{\mathrm{d}\varphi} = 0 \Rightarrow \tan\varphi = -k^2\,\frac{\sigma^0_{xz}}{\sigma^0_{yz}}, \quad \tan\theta = k\tan\varphi. \tag{37}$$

The maximum magnitude of τ is

$$|\tau|_{\max} = \left(1 + \frac{1}{k}\right)\left(\sigma^{02}_{yz} + k^2\sigma^{02}_{xz}\right)^{1/2}. \tag{38}$$

Along the congruent ellipse in a solid without a hole, the corresponding results are

$$\frac{\mathrm{d}\tau^0}{\mathrm{d}\varphi} = 0 \Rightarrow \tan\varphi^0 = -k\,\frac{\sigma^0_{xz}}{\sigma^0_{yz}}, \quad \tan\theta^0 = k\tan\varphi^0, \tag{39}$$

and

$$|\tau^0|_{\max} = \left(\sigma^{02}_{yz} + \sigma^{02}_{xz}\right)^{1/2}. \tag{40}$$

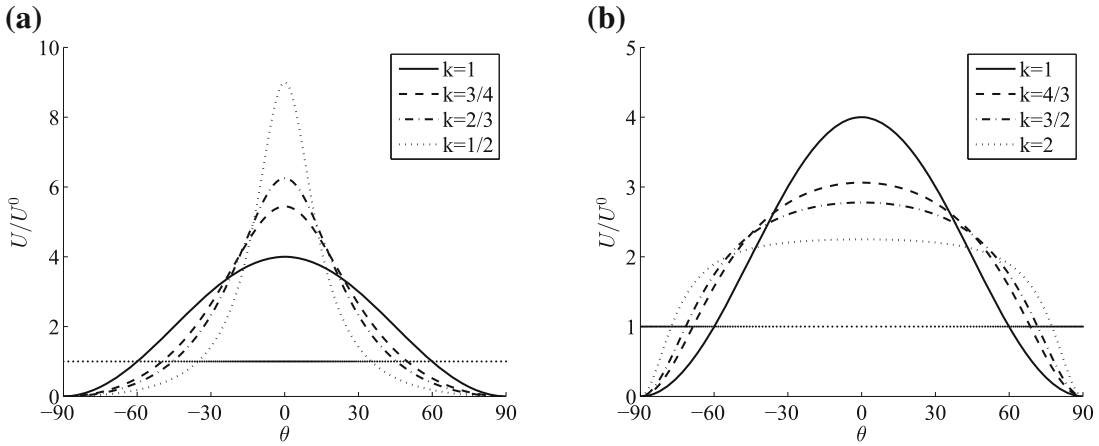

Fig. 6 The variation of the elastic strain energy density ratio U/U^0 under remote loading $\sigma^0_{yz} \neq 0$, $\sigma^0_{xz} = 0$ along the ellipse for: **a** four selected values of the ellipse aspect ratio $k = b/a$, and **b** their reciprocals

Thus, the angles at which the maximum circumferential shear stresses in two cases occur are related by $\tan\varphi = k\tan\varphi^0$, and

$$\frac{|\tau|_{\max}}{|\tau^0|_{\max}} = \left(1+\frac{1}{k}\right)\left(\frac{\sigma^{02}_{yz}+k^2\sigma^{02}_{xz}}{\sigma^{02}_{yz}+\sigma^{02}_{xz}}\right)^{1/2}. \tag{41}$$

In the case of remote shear loading $\sigma^0_{yz} \neq 0$, $\sigma^0_{xz} = 0$, the maximum shear stresses are $|\tau|_{\max} = (1+k^{-1})\sigma^0_{yz}$ and $|\tau^0|_{\max} = \sigma^0_{yz}$ (both at $x = \pm a$), reproducing the well-known stress concentration factor of $1+k^{-1}$ [18]. In the case $\sigma^0_{xz} \neq 0$, $\sigma^0_{yz} = 0$, the stress concentration factor is $1+k$. In the cases $\sigma^0_{yz} = \pm\sigma^0_{xz}$, we have

$$\frac{|\tau|_{\max}}{|\tau^0|_{\max}} = \left(1+\frac{1}{k}\right)\left(\frac{1+k^2}{2}\right)^{1/2}, \quad \frac{|\tau|_{\max}}{|\sigma^0_{yz}|} = \left(1+\frac{1}{k}\right)(1+k^2)^{1/2}, \tag{42}$$

with the maxima occurring at $\tan\varphi = \mp k^2$ for $|\tau|_{\max}$, and $\tan\varphi^0 = \mp k$ for $|\tau^0|_{\max}$.

4.1 Elastic strain energy around an elliptical hole

The elastic strain energy density along the boundary of the elliptical hole is $U = \tau^2/(2\mu)$, while the elastic strain energy along the congruent ellipse in a solid without a hole is $U^0 = (\sigma^{02}_{xz}+\sigma^{02}_{yz})/(2\mu)$. Thus, in view of (34), their ratio is

$$\frac{U}{U^0} = \frac{(1+k)^2\left(\sigma^0_{xz}\sin\varphi - \sigma^0_{yz}\cos\varphi\right)^2}{\left(\sigma^{02}_{xz}+\sigma^{02}_{yz}\right)\left(\sin^2\varphi + k^2\cos^2\varphi\right)}. \tag{43}$$

For example, if $\sigma^0_{xz} = 0$, the elastic strain energy ratio becomes

$$\frac{U}{U^0} = \frac{\tau^2}{\sigma^{02}_{zy}} = (1+k)^2\frac{\cos^2\varphi}{\sin^2\varphi + k^2\cos^2\varphi}. \tag{44}$$

The variation of U/U^0 around the boundary of the ellipse, for various values of k, is shown in Fig. 6. The inequalities $|\tau|/\sigma^0_{yz} \leq 1$ and $U/U^0 \leq 1$ hold for $\sec^2\varphi \geq 2(1+k)$, i.e., $\sec^2\theta \geq [1+k^2(1+2k)]$. The same curves correspond to $\sigma^0_{xz} \neq 0$, $\sigma^0_{yz} = 0$, provided that in both parts of the figure, (a) and (b), the values of k are replaced by their reciprocal values $1/k$.

Figure 7 shows the variation of U/U^0 around the boundary of the ellipse in the cases when the loading is $\sigma^0_{xz} = \sigma^0_{yz}$, and $\sigma^0_{xz} = -\sigma^0_{yz}$. The curves correspond to four selected values of the aspect ratio k. The curves

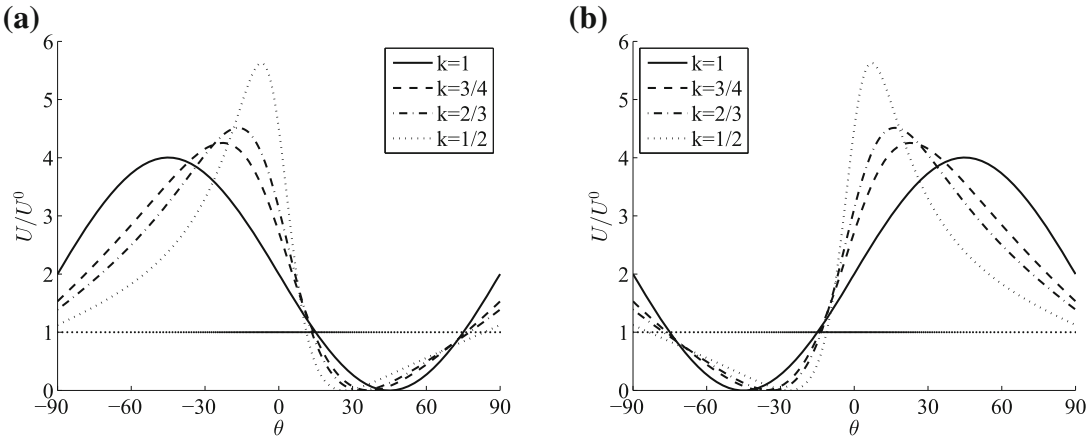

Fig. 7 The variation of the elastic strain energy density ratio U/U^0 under remote loading: **a** $\sigma^0_{xz} = \sigma^0_{yz}$, and **b** $\sigma^0_{xz} = -\sigma^0_{yz}$, for four selected values of $k \leq 1$

for the reciprocals of the selected values of k are obtained by mirror image of the shown curves across the vertical line $\theta = 45°$. The loading case $\sigma^0_{xz} = -\sigma^0_{yz}$ can be generated from the loading case $\sigma^0_{xz} = \sigma^0_{yz}$ by the counterclockwise rotation of the latter configuration with an angle of 90°.

For a circular hole, (43) simplifies to

$$\frac{U}{U^0} = \frac{4\left(\sigma^0_{xz}\sin\varphi - \sigma^0_{yz}\cos\varphi\right)^2}{\sigma^{02}_{xz} + \sigma^{02}_{yz}}. \tag{45}$$

The elastic strain energy density around a circular hole is not increased by the creation of a hole ($U \leq U^0$), if

$$4\sigma^0_{xz}\sigma^0_{yz} - \sqrt{3}\left(\sigma^{02}_{xz} + \sigma^{02}_{yz}\right) \leq \left(3\sigma^{02}_{xz} - \sigma^{02}_{yz}\right)\tan\varphi \leq 4\sigma^0_{xz}\sigma^0_{yz} + \sqrt{3}\left(\sigma^{02}_{xz} + \sigma^{02}_{yz}\right). \tag{46}$$

This gives $|\tan\varphi| \leq \sqrt{3}$ for $\sigma^0_{xz} = 0$, $|\tan\varphi| \leq \sqrt{3}/3$ for $\sigma^0_{yz} = 0$, and $\pm 2 - \sqrt{3} \leq \tan\varphi \leq \pm 2 + \sqrt{3}$ for $\sigma^0_{xz} = \pm\sigma^0_{yz}$. In the latter case, within the first and fourth quadrant, $15° \leq \varphi \leq 75°$ for $\sigma^0_{xz} = \sigma^0_{yz}$, and $-75° \leq \varphi \leq -15°$ for $\sigma^0_{xz} = -\sigma^0_{yz}$.

5 Circumferential shear stress around an inclined elliptical hole

The results from the previous section can be applied to determine the circumferential shear stress along the boundary of an inclined elliptical hole under antiplane shear loading σ^0 over remote horizontal planes as shown in Fig. 8. By aligning the x and y axes with the main axes of the ellipse, one has $\sigma_{xz} = \sigma^0\sin\alpha$ and $\sigma_{yz} = \sigma^0\cos\alpha$, and from (33) and (34) there follows

$$\tau = \frac{(1+k)\cos(\alpha+\varphi)}{\left(\sin^2\varphi + k^2\cos^2\varphi\right)^{1/2}}\,\sigma^0, \quad \tau^0 = \frac{k\cos\alpha\cos\varphi - \sin\alpha\sin\varphi}{\left(\sin^2\varphi + k^2\cos^2\varphi\right)^{1/2}}\,\sigma^0. \tag{47}$$

The maximum circumferential shear stresses are $|\tau^0|_{\max} = \sigma^0$ at $\tan\varphi_0 = -k\tan\alpha$, and

$$|\tau|_{\max} = \left(1 + \frac{1}{k}\right)\left(\cos^2\alpha + k^2\sin^2\alpha\right)^{1/2}\sigma^0, \tag{48}$$

at the angle defined by $\tan\varphi = -k^2\tan\alpha$. Consequently, the stress concentration factor (SCF) is

$$\mathrm{SCF} = \frac{|\tau|_{\max}}{\sigma^0} = \left(1 + \frac{1}{k}\right)\left(\cos^2\alpha + k^2\sin^2\alpha\right)^{1/2}, \tag{49}$$

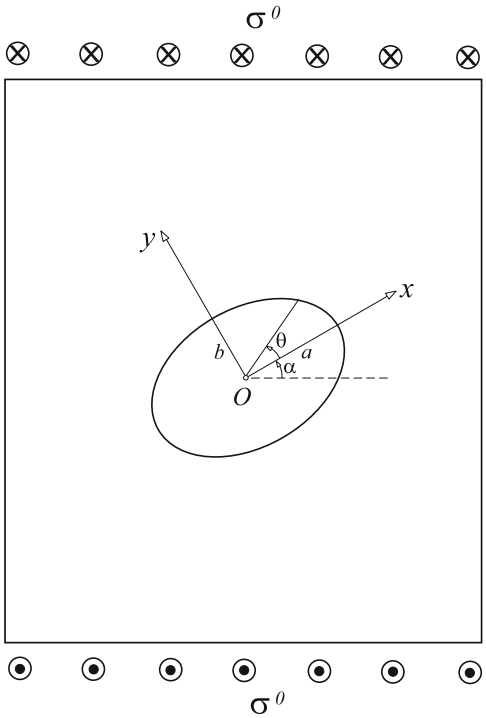

Fig. 8 An elliptical hole with the semi-axes a and b in an infinite solid under remote shear stress σ^0. The angle of inclination of the ellipse main axis x relative to the horizontal direction is α

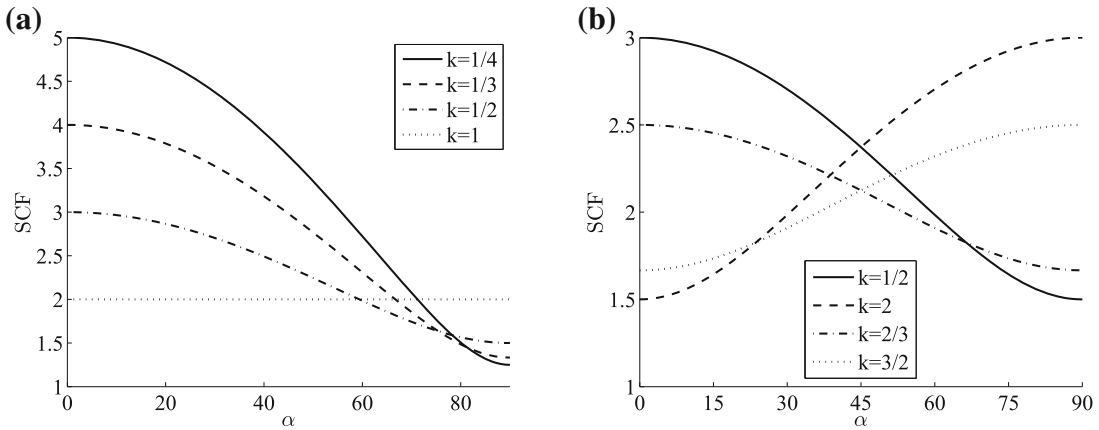

Fig. 9 Variation of the stress concentration factor SCF with the inclination angle α for: **a** four selected values of the ellipse aspect ratio $k = b/a$, and **b** for two selected values of k and their reciprocals

which is plotted for the selected values of the aspect ratio k versus the angle α in Fig. 9a. In particular, for $\alpha = 0°,\ 45°,\ 90°$, the stress concentration factor is

$$\mathrm{SCF}(0°) = 1 + \frac{1}{k}, \quad \mathrm{SCF}(45°) = \left(1 + \frac{1}{k}\right)\left(\frac{1+k^2}{2}\right)^{1/2}, \quad \mathrm{SCF}(90°) = 1 + k. \tag{50}$$

The plots of SCF for $k = 1/2$ and $2/3$, and their reciprocals, are shown in Fig. 9b.

The expression for the stress concentration factor SCF under antiplane shear loading over remote vertical planes is obtained from (49) by replacing α with $90° - \alpha$, or k with $1/k$; both give

$$\mathrm{SCF} = \left(1 + \frac{1}{k}\right)\left(\sin^2\alpha + k^2\cos^2\alpha\right)^{1/2}. \tag{51}$$

For each angle α, the SCF for the ellipse with the aspect ratio k, under shear loading over remote horizontal planes, is equal to the SCF for the ellipse with the aspect ratio $1/k$, under shear loading over remote vertical planes.

6 Conclusions

The circumferential shear stress formula, deduced by Lin et al. [1] from the extended circle theorem of Milne-Thomson, is rederived in this paper using the Fourier series analysis, analogously to the Kienzler and Zhuping [2] derivation of the plane strain version for the hoop stress around a circular hole. The shear stress formula is also derived using the complex potential approach, without explicitly invoking the extended circle theorem. According to this formula, the circumferential shear stress along the boundary of a traction-free circular hole in an infinite isotropic solid under antiplane shear loading is twice the circumferential shear stress along the corresponding circle in an infinite solid without a hole, under the same loading conditions. For noncircular holes, the ratio of the circumferential shear stress along the boundary of the hole and a congruent curve in an infinite solid without a hole depends on the loading. For an elliptical hole under remote loading σ^0_{xz}, the stress ratio is constant and equal to $1 + b/a$; under remote σ^0_{yz} loading it is equal to $1 + a/b$, where a and b are the semi-axes of the ellipse. These constant values coincide with the values of the stress concentration factor in the two cases. If σ^0_{xz} and σ^0_{yz} are both applied, the stress ratio varies along the boundary of the ellipse. A closed form expression for this variation is determined. The change in the elastic strain energy density along the boundary of the ellipse, produced by the creation of the hole, is determined for different types of loading and different aspect ratios of the ellipse. The stress concentration factor is also evaluated for an arbitrary orientation of the ellipse relative to the applied load. The analysis for other types of loading, such as internal sources of stress, can be performed similarly. For example, the complex potential for a screw dislocation of the Burgers vector b_z, with the dislocation center at the point $\zeta_0 = d\exp(i\varphi)$, relative to the center of a circular hole of radius R in the ζ-plane, is $\Omega = (\mu b_z/2\pi)\ln[\zeta(\zeta - \zeta_0)/(\zeta - (R^2/d^2)\zeta_0)]$, and the conformal mapping (27) yields the stresses for a screw dislocation near an elliptical hole according to (28). The interaction of screw dislocation with circular, elliptical, or arbitrarily shaped holes and elastic inhomogeneities by means of conformal mapping has been previously studied in [22–24]. The stress concentration factors in certain types of functionally graded plates or panels, weakened by a circular hole and subjected to antiplane shear loading, have been recently evaluated in [25,26].

Acknowledgments Research support from the Montenegrin Academy of Sciences and Arts is gratefully acknowledged. I also thank the reviewers for their helpful comments and suggestions.

References

1. Lin, W.-W., Honein, T., Herrmann, G.: A novel method of stress analysis of elastic materials with damage zones. In: Boehler, J.P. (ed.) Yielding, Damage, and Failure of Anisotropic Solids. EGF Publication 5, pp. 609–615. Mechanical Engineering Publications, London (1990)
2. Kienzler, R., Zhuping, D.: On the distribution of hoop stresses around circular holes in elastic sheets. J. Appl. Mech. **54**, 110–114 (1987)
3. Honein, T., Herrmann, G.: The involution correspondence in plane elastostatics for regions bounded by circle. J. Appl. Mech. **55**, 566–573 (1988)
4. Honein, T., Herrmann, G.: On bonded inclusions with circular or straight boundaries in plane elastostatics. J. Appl. Mech. **57**, 850–856 (1990)
5. Milne-Thomson, L.M.: Hydrodynamical images. Proc. Camb. Philos. Soc. **36**, 246–247 (1940)
6. Milne-Thomson, L.M.: Theoretical Hydrodynamics (5th edn). Macmillan Press, London (1968)
7. Smith, E.: The interaction between dislocations and inhomogeneities—I. Int. J. Eng. Sci. **6**, 129–143 (1968)
8. Honein, E., Honein, T., Herrmann, G.: On two circular inclusions in harmonic problems. Q. Appl. Math. **50**, 479–499 (1992)
9. Honein, E., Honein, T., Herrmann, G.: Further aspects on the elastic field for two circular inclusions in antiplane elastostatics. J. Appl. Mech. **59**, 774–779 (1992)
10. Honein, E., Honein, T., Herrmann, G.: Energetics of two circular inclusions in anti-plane elastostatics. Int. J. Solids Struct. **37**, 3667–3679 (2000)
11. Kienzler, R., Kordisch, H.: Calculation of J_1 and J_2 using the L and M integrals. Int. J. Fracture **43**, 213–225 (1990)
12. Greenwood, J.A.: Stresses around a circular hole in a uniform bar in tension. J. Appl. Mech. **61**, 213–214 (1994)
13. Golecki, J.J.: On stress concentration around circular holes. Int. J. Fract. **73**, R15–R17 (1995)
14. Chao, C.K., Heh, T.Y.: Thermoelastic interaction between a hole and an elastic circular inclusion. AIAA J. **37**, 475–481 (1999)
15. Kienzler, R., Fischer, F.D., Fratzl, P.: On energy changes due to the formation of a circular hole in an elastic plate. Arch. Appl. Mech. **76**, 681–697 (2006)

16. Lubarda, V.A.: Interaction between a circular inclusion and void under plane strain conditions (2014, under review)
17. Lubarda, V.A.: Circular inclusion near a circular void: determination of elastic antiplane shear fields and configurational forces. Acta Mech. (2014. doi: 10.1007/s00707-014-1219-9)
18. Suo, Z.: Advanced Elasticity: Complex variable methods. Lecture Notes, http://imechanica.org. Harvard University (2009)
19. Muskhelishvili, N.I.: Some Basic Problems of the Mathematical Theory of Elasticity. P. Noordhoff, Groningen (1953)
20. Kanninen, M.F., Popelar, C.H.: Advanced Fracture Mechanics. Oxford Engineering Science Series 15. Oxford University Press, New York (1985)
21. Broberg, K.B.: Cracks and Fracture. Academic Press, New York (1999)
22. Gong, S.X., Meguid, S.A.: A screw dislocation interacting with an elastic elliptical inhomogeneity. Int. J. Eng. Sci. **32**, 1221–1228 (1994)
23. Müller, W.H., Kemmer, G.: Applications of the concept of J-integrals for calculation of generalized forces. Acta Mech. **129**, 1–12 (1998)
24. Wang, X., Sudak, L.J.: Interaction of a screw dislocation with an arbitrary shaped elastic inhomogeneity. J. Appl. Mech. **73**, 206–211 (2006)
25. Kubair, D.V.: Stress concentration factors and stress-gradients due to circular holes in radially functionally graded panels subjected to anti-plane shear loading. Acta Mech. **224**, 2845–2862 (2013)
26. Kubair, D.V.: Stress concentration factor in functionally graded plates with circular holes subjected to anti-plane shear loading. J. Elast. **114**, 179–196 (2014)